



ORIGINAL ARTICLE

Fatigue behavior and calculation methods of high strength steel fiber reinforced concrete beam

Zhiqiang Gu^a, Hu Feng^a, Danying Gao^{a*}, Jun Zhao^b, Congjie Wei^c, Chenglin Wu^c

^aYellow River Laboratory, Zhengzhou University, Zhengzhou, 450001, China.

^bSchool of Water Conservancy and Civil Engineering, Zhengzhou University, Zhengzhou, 450001, China.

^cDepartment of Civil, Architectural, and Environmental Engineering, Missouri University of Science and Technology, Rolla, MO, USA.

*Corresponding Author: Danying Gao. Email: gaodanyingzzu@126.com.

Abstract: Adding steel fibers into concrete was considered as one of the most effective ways to restrain the crack development and improve the stiffness for reinforced concrete (RC) structures. To explore the reinforcement mechanism of steel fibers on the fatigue behavior of high-strength RC beam, eight high-strength steel fiber reinforced concrete (HSSFRC) beams subjected to fatigue loading were tested in this study. The main design parameters considered in this work were stress level and steel fiber content. The failure mode, crack patterns, fatigue life, crack width, and stiffness degradation of HSSFRC beams under fatigue loading were discussed. The results showed that steel fibers could significantly increase the fatigue life, restrain crack development, and improve crack patterns of HSSFRC beams under fatigue loading compared to ordinary RC beams. Both the crack width and stiffness degradation rate of beams decrease with increasing steel fiber content. Besides, the empirical formulas for calculating the maximum crack width and midspan deflection of HSSFRC beam under fatigue loading were proposed and validated using experimental results.

Keywords: Fatigue behavior; flexural beam; high-strength SFRC; crack width calculation; midspan deflection calculation

1 Introduction

Due to the high bearing capacity, high resistance to deformation ability, and good formability, reinforced concrete (RC) structures have received much attention in engineering construction. Except for static loading, part of RC structures such as bridge, high-speed railway, and airport runway would also subject to fatigue loading [1]. Existing research indicated that the brittle fracture of tensile reinforcement was the principal reason that causes the failure of these structures under fatigue loading [2, 3]. While studies have shown that the stress concentration of RC structures at tension cracks was the main cause of reinforcement fatigue fracture [4, 5]. Therefore, cracks have an obvious influence on the RC structures under fatigue loading.

However, concrete was easy cracking due to the brittleness. To improve the toughness of concrete, numerous research had been conducted in the past decades. Adding fiber was considered as one of the most effective methods [6, 7]. The bridging stresses provide by fibers could restrain crack development and improve stress concentration at crack tips, which lead to the increasing toughness of concrete [8-10]. The existing studies indicated that steel fibers could effectively slow down the crack growth rate



of concrete under fatigue loading [11]. The crack propagation of pre-cracked concrete was restrained by adding steel fibers [12]. Steel fibers could significantly increase the fatigue life of concrete under bending or tension fatigue loads [13-17]. Nowadays, recycling of construction and building (C&D) waste have received much attention. However, due to the existence of weak interfacial transition zones and high porosity of recycled aggregates, recycled concrete has poor mechanical properties and durability [18]. While adding steel fibers was one of the most effective way to achieve the recycling of C&D waste [19]. Existing research indicates that the mechanical properties of recycled concrete could be significantly improved by adding steel fibers, both under static and fatigue loading. Gao et al. [20-22] conducted a series of research about steel fiber reinforced recycled concrete under static loading. The results showed that both the flexural, shear, and tensile strength of recycled concrete could be improved by adding steel fibers. Tan [23] conducted the flexural fatigue test of steel fiber reinforced recycled aggregate concrete. Results showed that by adding 1.0% volume fraction of steel fibers, the flexural strength of recycled concrete was bigger than that of the ordinary concrete. Moreover, compared to ordinary concrete, the fatigue life of steel fiber reinforced recycled concrete at a stress level of 0.7 was increased by 53.4%. Therefore, except for improving the mechanical properties of concrete, steel fibers can also contribute to the sustainable development of concrete resources.

In recently decades, the fatigue performance of SFRC structures has also gained attention. Parvez [24] conducted the flexural fatigue test of SFRC beams and found that the main reason for the increasing fatigue life of SFRC beam is that the bridging stress provided by the steel fibers in the tension region decreases the fatigue stress of tensile reinforcement. Gao [25, 26] reported that steel fibers could positively affect the stress concentration of beams subjected to fatigue loading, and improve the crack patterns, stiffness, and fatigue life significantly. Isojeh [27, 28] studied the shear fatigue resistance of SFRC deep beam. The findings indicated that steel fibers could increase the fatigue life as well as restrain the crack and deflection growth of SFRC deep beams. Mohamed [29] analyzed the stress degradation of SFRC in the tension zone of beams under flexural fatigue loading. Test results showed that higher SFRC strength resulted in a longer fatigue life and lower crack-bridging degradation rates for SFRC beams.

From the above research, it could be concluded that steel fibers could improve the fatigue behavior of ordinary concrete, recycled concrete, and reinforced concrete structures. Moreover, the improvements were more significant for high strength concrete. However, most of the studies mentioned above are based on ordinary strength concrete that does not exceed 60 MPa. The fatigue behavior of high-strength SFRC and its structures with concrete strength exceeding 80 MPa has been rarely studied.

In recent decades, with the development of building structures to the direction of high-rise and long-span, the higher requirements were proposed for the concrete performance. High-strength concrete (HSC), with its properties of high strength, low shrink age, and high durability, has been increasingly applied to building structures [30]. However, the higher strength increased the brittleness of concrete, resulted in excessive cracking of RC structures under high stress level [31]. Adding steel fibers into HSC was a good choice to improve the toughness of structures, which could meet the applicability and durability requirements of structures under serviceability limit state. The inclusion of steel fibers into HSC beams improved the stiffness and consequently decreased the deflection of RC members [32]. Liu [33] conducted the fatigue test of pre-stressed high strength steel fiber reinforced concrete (HSSFRC) beams. Test results showed that steel fibers could improve the crack resistance of fully pre-stressed HSSFC beams significantly. The improvements of steel fibers on the stiffness and fatigue life of fully pre-stressed HSSFC beams were better than that of the partially pre-stressed HSSFC beams. Besides, several scholars have studied the shear behavior of HSSFRC beam subjected to static loading [34-36]. Results showed that steel fibers can significantly inhibit the crack propagation and produce more diffused flexural cracks for HSSFRC beams. The HSSFRC beams without stirrup exhibited the similar shear behavior to that of plain HSC beams containing stirrup reinforcement.

Nowadays, the HSC has been used in RC structures that subjected to fatigue loading. It could be seen that adding steel fibers into these structures could significantly improve its fatigue performance. While the studies on the fatigue behavior of HSSFRC structures has not received much attention. Besides, the crack and deflection are important indexes for evaluating structural behavior, the crack and

deflection calculation methods for SFRC beams under static loading have been introduced into the related specifications [37, 38]. However, the crack and deflection calculation methods for HSSFRC beam subjected to fatigue loading, especially the empirical calculation formulas that applicable to engineering design, are rarely reported. The calculation methods to predict crack width and deflection of HSSFRC beams under fatigue loading are urgently needed to provide a reference for engineering design.

Upon this background, eight HSSFRC beams were prepared in this study. The fatigue life, failure mode, crack patterns, crack width, and stiffness of HSSFRC beams including were first discussed. Then, the calculation methods to predict the maximum crack width and midspan deflection of HSSFRC beams under fatigue loading were proposed. The relevant research results can provide a reference for the application of HSSFRC in structures subjected to fatigue loading.

2 Test program

2.1 Materials

Portland cement with the 28-days compressive strength of 42.5 MPa was used as cementitious materials. The coarse aggregates were natural gravel with a continuous grading of 5-20 mm. River sand with the fineness modulus of 2.8 was used as fine aggregates. Liquid polycarboxylic acid water reducer was used in this work, and its water reducing rate was 20%. The HSSFRC mix proportion in this study was the same of 1:2.1:1.2:0.08 (cement: coarse aggregate: fine aggregate: superplasticizer by weight), and the steel fibers were added in the mixture by volume fraction of 0, 0.5%, 1.0%, 1.5%. The picture of steel fibers is presented in **Fig. 1**. The length of steel fiber was 35 mm with the aspect ratio of 64. The steel fibers have an elastic modulus of 200 GPa and ultimate tensile strength of 1345 MPa. The target compressive strength grade of HSSFRC in this work was designed as C80. The tensile reinforcements used in this work were 12 mm diameter ribbed steel bar, and it has a yield strength of 585 MPa (HRB500) and ultimate tensile strength of 705 MPa. The compression reinforcements and stirrups used in this work were 8 mm diameter plain steel bar, and it has a yield strength of 425 MPa (HPB300) and ultimate tensile strength of 550 MPa. The fabricated steel reinforcement cage is shown in **Fig. 2**.

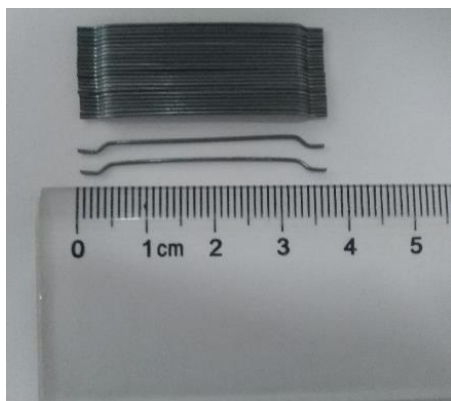


Fig. 1. Picture of steel fiber.



Fig. 2. Reinforcement cage of the beam.

2.2 Specimen design

Table 1 listed the design parameters of the HSSFRC beam and mechanical properties of concrete. All beams were demoulded 24 hours after pouring, and then placed in the standard maintenance environment with the humidity of 95% and temperature of 20 ± 2 °C for 28 days. After that, the beams were placed indoors for three months to avoid the influence of later concrete strength growth on the fatigue test results. Beam BJ1.0-5 was applied the monotonic quasi static load to failure to provide reference for load amplitude of fatigue test beam. Because of the limitations of time and test condition, the high stress levels were applied on the fatigue test beams. If the fatigue test beam has not experienced fatigue failure after 2 million fatigue cycles, it is considered that the test beam will not fail under this stress level and then the static load will apply until it failed. In this test program, the stress level was set

as the ratio of upper limit fatigue loads to the ultimate load capacity of HSSFRC beams. The lower limit fatigue loads were set as 0.1 times of the ultimate load capacity for all beams. Besides, the target compressive strength grade designed in this work was based on HSSFRC with the steel fiber volume fraction of 1.0%. Therefore, the compressive strength of beams BF0-6 and BF0.5-6 was relatively lower.

Table 1. Design parameters and mechanical properties of the HSSFRC beams.

Specimen ID	Test type	Stress level	Steel fiber volume fraction (%)	Mechanical properties of concrete		
				f_{st}^a (MPa)	f_{cu}^b (MPa)	E_c^c (MPa)
BJ1.0-5	Static	–	1.0	87.6	5.88	41.6
BS1.0-5	Fatigue	0.5	1.0	83.4	6.37	40.8
BS1.0-6	Fatigue	0.6	1.0	87.6	5.88	41.6
BS1.0-7	Fatigue	0.7	1.0	85.7	6.28	39.4
BS1.0-8	Fatigue	0.8	1.0	86.3	6.35	42.4
BF0-6	Fatigue	0.6	0	75.4	3.69	37.1
BF0.5-6	Fatigue	0.6	0.5	79.9	5.15	40.8
BF1.5-6	Fatigue	0.6	1.5	85.6	7.97	42.2

f_{st}^a : splitting tensile strength, f_{cu}^b : compressive strength, E_c^c : elastic modulus of concrete

2.3 Testing equipment and instrumentation

All beams in this work were implemented on the 500 kN fatigue testing machine. **Fig. 3** presents the support mode, load span length, section dimension, reinforcement details, steel strain gauges and linear variable differential transformers (LVDTs) arrangements of HSSFRC beams. The loading rate of the beam BJ1.0-5 was set as 0.2 mm/min up to failure. The fatigue test was implemented by load control mode with a constant amplitude sinusoidal wave. The fatigue loading frequency was set as 5 Hz.

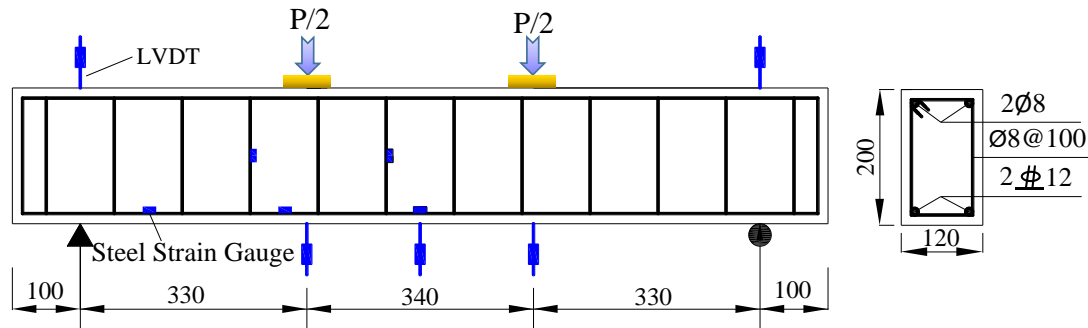


Fig. 3. Loading diagram of beam.



Fig. 4. Experimental setup.

The strains of tensile reinforcements and stirrups of beams were measured by electrical resistance strain gages, and the midspan deflection was measured by LVDT, as shown in Fig. 3. Fig. 4 presents the experimental setup. For fatigue test beam, the static tests were implemented at the certain number of cycles for data recording and observation during the fatigue loading. During each static test, the strains measured by electrical resistance strain gages and midspan deflections measured by LVDT were recorded using the data collecting instrument, the crack development of beams was marked using the black pen, and the crack width of the beams at the location of the tensile reinforcement was measured using the crack width detector. The measurement range of the crack width detector was 2 mm and measurement accuracy 0.02 mm. Because of the typical brittle failure mode of fatigue test beams, which occurs without warning, the crack and midspan deflection data at the stage when the beam is close to failure were not detected in this work.

3. Results and discussions

3.1 Failure modes and crack patterns of HSSFRC beams

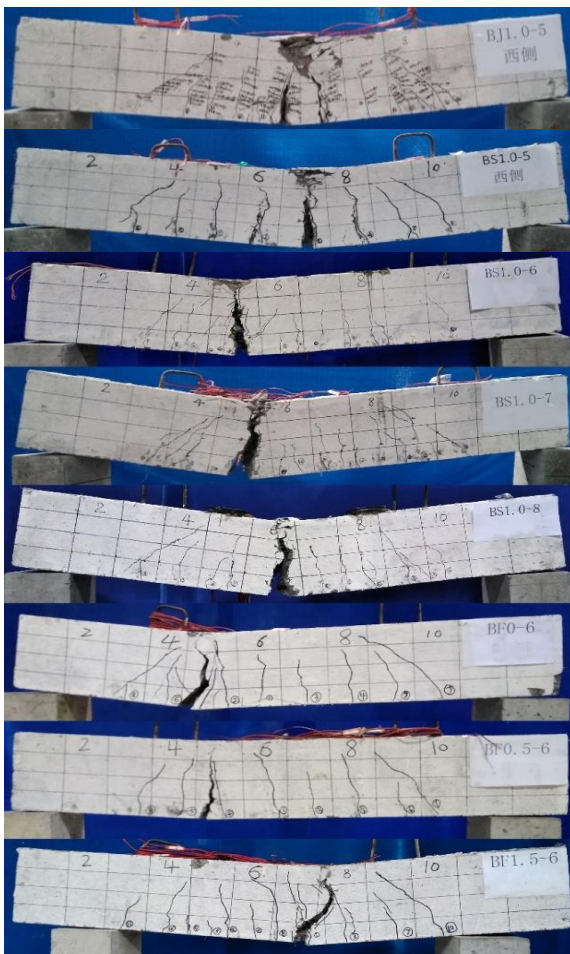


Fig. 5. Failure picture of beams.

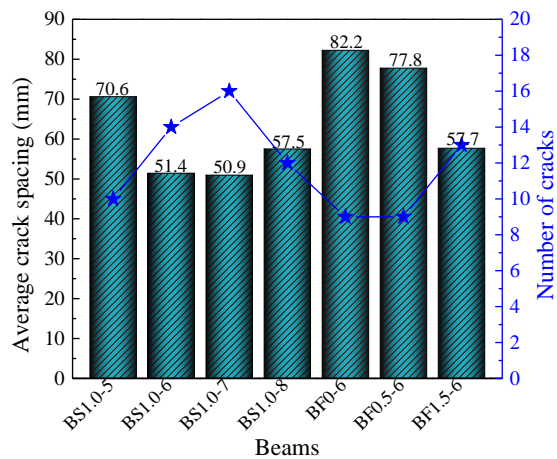


Fig. 6. Number of cracks and average crack spacing of fatigue test beams.

The final failure picture of beams is presented in Fig. 5. For static test beam, the failure mode is typical tension-controlled failure. In the initial loading stage, the midspan deflection showed a linearly increasing trend with the increasing load. Meanwhile, few diffused flexural cracks propagated in the pure bending section of beams. As the load further increases, a small amount of shear diagonal cracks appeared in the shear span section of beams. When the load reached approximately 0.85 times the ultimate load capacity of the beam, the width of main cracks increased quickly and the tensile reinforcement began yield. Subsequently, the concrete in compression zone reached its ultimate compression strain and crushed, while the load capacity of the beams slowly decreases until failure.

The fatigue test beam BS1.0-5, which did not fail after undergoing 2 million fatigue cycles and finally failed by static loading, exhibited a similar failure mode to that of the beam BJ1.0-5. While the other fatigue test beams were typical brittle failure without warning. For fatigue test beams, the crack nucleation firstly formed on the surface of tensile reinforcement due to the stress concentration, and then the micro-crack of tensile reinforcement propagated with the increasing fatigue cycles [39]. When the fatigue crack of tensile reinforcement propagated to a point where the reinforcement cannot bear the upper limit fatigue load, the HSSFRC beams came into the instability stage and failed quickly. According to the experimental observation, one tensile reinforcement first experienced brittle fracture, and then the other tensile reinforcement cannot bear the maximum fatigue load and finally resulting in the failure of beam quickly. It could be observed from **Fig. 5** that only one crack almost run through the whole beam section while the concrete in compression zone kept intact for all fatigue test HSSFRC beams.

Fig. 6 presents the number of cracks and average crack spacing of the fatigue test HSSFRC beams. For the beams subjected to different stress levels, the number of cracks and average crack spacing were relatively random and lack of regularity. While for different fiber content beams, the average crack spacing showed a decreasing trend with the increase in steel fiber content. Compared with the plain HSC beam, the average crack spacing of HSSFRC beams with 0.5%, 1.0%, and 1.5% steel fiber volume fractions were decreased by 5.4%, 37.5%, 29.8%, respectively. The main reason was that steel fibers not only increased the tensile strength of HSC, but also improved the bonding stress between reinforcement and HSC [40]. Therefore, the cracks of HSSFRC beams become thinner and denser.

3.2 Fatigue life and S-N curve of HRB500 bars in HSSFRC beams

Fig. 7 presents the fatigue life of HSSFRC beams. The beam BS1.0-5 did not fail under fatigue loading and finally failed under static loading. As shown, the fatigue life of HSSFRC beams was negatively correlated to stress level while positively correlated to steel fiber content. The fatigue life of beams BS1.0-6, BS1.0-7, and BS1.0-8 were 56.5%, 79.6%, and 96.7% less than that of the beam BS1.0-5. This could be explained by that the increasing stress level results in the increased fatigue stress of tensile reinforcement. While the fatigue life of beams BF0.5-6, BS1.0-6, and BF1.5-6 was 37.7%, 106.3%, and 61.4% greater than that of the plain HSC beam BF0-6. This could be explained by that the bridging stress provided by steel fiber at crack location could improve the stress concentration and decrease the fatigue stress of tensile reinforcement significantly. Besides, it should be noted that the fatigue life of beam BF1.5-6 was less than that of beam BS1.0-6. The main reason was that excessive steel fiber can lead to fiber clustering within the concrete, thus resulting in degradation of bonding properties between fibers and concrete matrix [41]. This phenomenon is more pronounced for HSC because of the lower water-cement ratio, which makes it more difficult to uniformly disperse the fibers in the concrete mixture during the mixing process. Therefore, beam BF1.5-6 exhibited a lower fatigue life. And the optimal fiber volume fraction for HSSFRC beams under fatigue loading should not exceed 1.0%.

According to the test results of tensile reinforcement strains, the average stress of tensile reinforcement of HSSFRC beams could be obtained. The stress amplitude $\Delta\sigma$ of tensile reinforcement at first fatigue cycle and the fatigue life N of beams are presented in **Fig. 8**. It could be seen that the fatigue life of HSSFRC beams is linearly related to the stress amplitude of tensile reinforcement on double-Log plots. The expression of stress-fatigue life (S-N) curve of HRB500 steel bars reinforced in the HSSFRC beams are given as follows:

$$LgN = 17.2Lg\Delta\sigma - 4.5 \quad (1)$$

where $\Delta\sigma = \sigma_{max} - \sigma_{min}$, σ_{max} and σ_{min} are the maximum and minimum fatigue stresses of tensile reinforcement at first fatigue cycle, respectively.

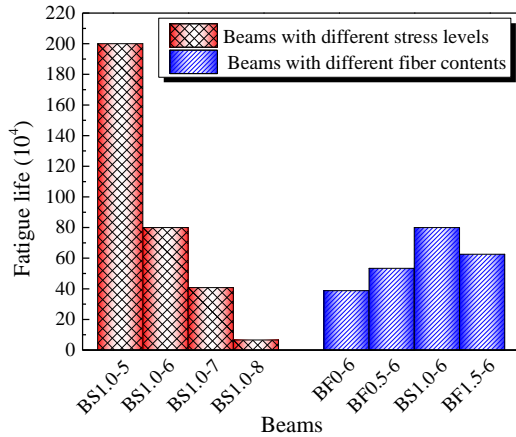


Fig. 7. Fatigue life of beams.

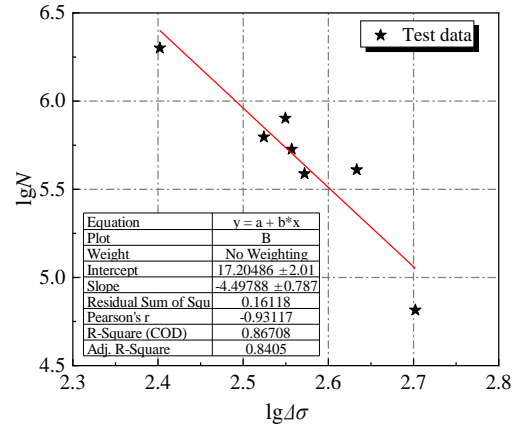
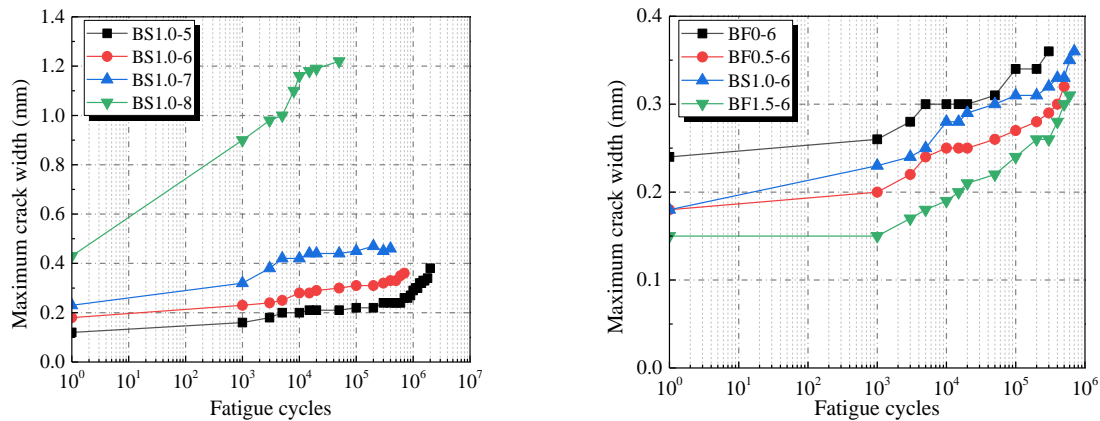


Fig. 8. S-N curve of tensile reinforcement.

3.3 Maximum and average crack widths of HSSFRC beam

Fig. 9 plots the relationship curves between the maximum crack widths of HSSFRC beams with the fatigue cycles. It could be observed that the maximum crack width was positively correlated to the stress level while negatively correlated to the steel fiber volume fraction. Take maximum crack width of beams subjected to different stress levels at 50,000 cycles for comparison, the beams BS1.0-6, BS1.0-7, and BS1.0-8 were 25%, 83.8%, and 408.3% bigger than that of the beam BS1.0-5. While the maximum crack width of beams BF0.5-6, BS1.0-6, and BF1.5-6 at 50,000 cycles was 19.2%, 3.3%, and 40.9% smaller than that of the plain HSC beam BF0-6. It should be noted that the maximum crack width of beam BS1.0-6 was bigger than that of beam BF0.5-6. The main reason is that the formation of crack is random. During the pouring process, internal defects may have occurred in the test beam BS1.0-6, resulting in stress concentration at this location and a significant increase in the maximum crack width. Besides, the tensile reinforcement of beam BS1.0-8 maybe yielded during the fatigue loading owing to the higher stress level, and therefore its maximum crack widths were significantly bigger than that of the other beams.



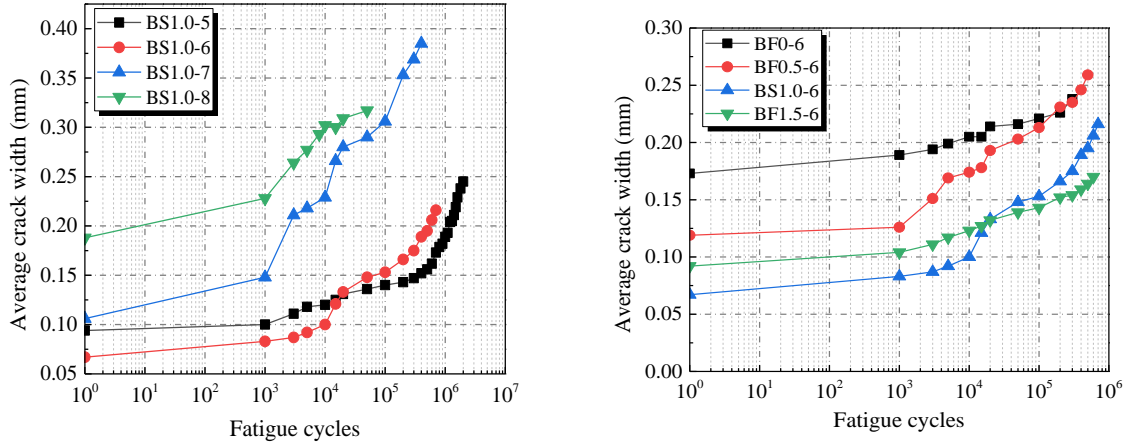
(a) Beams with different stress levels

(b) Beams with different steel fiber contents

Fig. 9. The relationship curves between the maximum crack width and the fatigue cycles.

Fig. 10 plots the relationship curves between the average crack widths of HSSFRC beams with the fatigue cycles. As shown, the average crack width of beams was positively correlated to the stress level while negatively correlated to the steel fiber volume fraction, which presented similar development trend with that of the maximum crack width of beams. Table 2 lists the average crack width reduction of beams with different steel fiber volume fractions at different fatigue cycles for comparison.

Compared with the plain HSC beam BF0-6, the reduction of the average crack width of the beam BF0.5-6 that reinforced with 0.5% fiber was not significant and even increases at 200,000 cycles. While with further increase of steel fiber content, the average crack width of beams decreased obviously. Compared to the plain HSC beam BF0-6, the reduction of the average crack width of the beam BF1.5-6 that reinforced with 0.5% fiber was exceeded 30%, which verified the effectiveness of steel fiber in restraining the crack development of HSSFRC beams.



(a) Beams with different stress levels

(b) Beams with different steel fiber contents

Fig. 10. The relationship curves between the average crack width and the fatigue cycles.

Table 2. Average crack width reduction of HSSFRC beams.

Specimen ID	50,000 cycles		100,000 cycles		200,000 cycles	
	Average width (mm)	Reduction (%)	Average width (mm)	Reduction (%)	Average width (mm)	Reduction (%)
BF0-6	0.216	—	0.221	—	0.226	—
BF0.5-6	0.203	6	0.213	3.6	0.231	-2.2
BS1.0-6	0.148	31.4	0.153	30.8	0.166	26
BF1.5-6	0.139	35.6	0.143	35.3	0.152	32

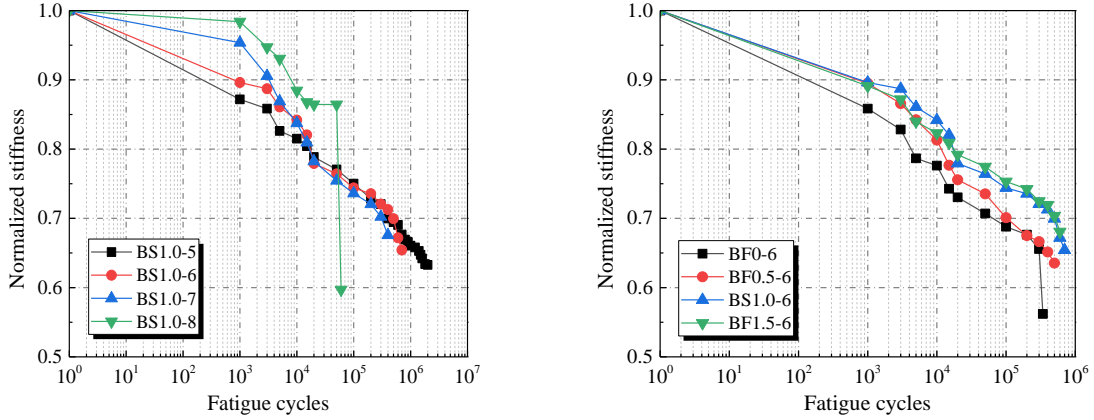
3.4 Stiffness degradation of HSSFRC beam

According to the tested results of midspan deflection of HSSFRC beam under fatigue loading, the stiffness of beams could be calculated as follows [42]:

$$B = \frac{P_{max} S}{48f} (3L^2 - 4S^2) \tag{2}$$

where P_{max} is the upper limit fatigue load; L is the clear span length of the beam; S is the shear span length of the beam; f is the midspan deflection of the beam.

To explore the stiffness degradation law of HSSFRC beams under fatigue loading, the normalized stiffness that defined as the ratio of the stiffness of the HSSFRC beam at the n th fatigue cycle to that of the first cycle was used in this paper. **Fig. 11** presents the relationship between the normalized stiffness with the fatigue cycles. It can be seen from **Fig. 11(a)** that the normalized stiffness decreased with the increase of fatigue cycles. For beams subjected to different stress levels, the normalized stiffness degradation rate of beams decreased with the increase in stress level. This could be explained by that the higher stress level will result in larger midspan deflection of beams in the first cycle, and the stiffness of beams in first cycle decreases as well. Therefore, the normalized stiffness degradation rate of beams subjected to higher stress level was relatively small. For different steel fiber content beams that subjected to the same stress level, the normalized stiffness degradation rate decreased with the increase in steel fiber content. It could be concluded that the stiffness degradation of HSC beams subjected to fatigue loading could be effectively restrained by adding steel fibers.



(a) Beams with different stress levels

(b) Beams with different steel fiber contents

Fig. 11. Relationship between the normalized stiffness degradation with the fatigue cycles.

4. Maximum crack width calculation of the HSSSFRC beam

4.1 Maximum crack width calculation of HSSFRC beam subjected static load

Existing studies [43, 44] indicated that the load types, mechanics characteristic, reinforcement ratio, reinforcement strength, and concrete cover thickness are main factors that affecting the crack width of RC beams. Based on the Chinese standard GB 50010-2010 [45], for RC beams under the standard combination loads that considered the long-term load effects, the maximum crack width could be calculated as follows:

$$\omega_{\max} = \alpha_{cr} \psi \frac{\sigma_s}{E_s} (1.9c_s + 0.08 \frac{d_{eq}}{\rho_{te}}) \quad (3)$$

$$\psi = 1.1 - 0.65 \frac{f_{tk}}{\rho_{te} \sigma_s} \quad (4)$$

$$\sigma_s = M / (0.87 A_s h_0) \quad (5)$$

$$\rho_{te} = \frac{A_s}{A_{te}} \quad (6)$$

$$d_{ep} = \frac{\sum n_i d_i^2}{\sum n_i d_i v_i} \quad (7)$$

where $\alpha_{cr} = 1.4$ is the mechanics characteristic parameter of high-strength RC members subjected to bending moment [46]; c_s is the concrete cover thickness; f_{tk} is axial tensile strength of concrete; A_s is the cross-sectional area of tensile reinforcement; M is the bending moment applied on the beam; h_0 is the effective height of beam; A_{te} is the effective concrete tensile area and taken as half of the beam section area; E_s is the elastic modulus of tensile reinforcement; d_i is the diameter of the longitudinal tensile reinforcement for the i th type (i is a variable representing the number of types of longitudinal tensile reinforcement, and the meaning of the following i is the same); n_i is the number of the longitudinal tensile reinforcement for the i th type; $v_i = 1.0$ is relative adhesion characteristic coefficient of longitudinal tensile reinforcement for the i th type.

As mentioned above, steel fibers could decrease the maximum crack width and restrain the crack development of RC beam remarkably. Therefore, the influences of steel fibers should be take into consideration for crack width calculation of SFRC beam [47]. For SFRC beams under static loading, the maximum crack width can be calculated as follows [38]:

$$\omega_{f \max} = \omega_{\max} (1 - \beta_{cw} \lambda_f) \quad (8)$$

$$\lambda_f = \frac{l_f}{d_f} V_f \quad (9)$$

where β_{cw} is the coefficient that considered the influence of steel fiber; l_f , d_f , and V_f are the length, diameter, and volume fraction of steel fibers, respectively.

For SFRC flexural members with the concrete compressive strength not exceed 45 MPa, β_{cw} was taken as 0.35 [38]. The value of β_{cw} increases with the increase in concrete strength because of the restrain effect of steel fibers on the crack development was more obvious for HSC beams [48]. According to the test results of 7 specimens in this work and 16 SFRC beams with the concrete compressive strength exceed 60 MPa from other literatures [46, 48], the coefficient β_{cw} of HSSFRC beam was taken as 0.65 through linear regression analysis. The calculation and test maximum crack widths of 23 HSSFRC beams under different service loads are presented in Fig. 12. As shown, the average ratio (AVG) of the calculation results to the test results was 1.1, and the coefficient of variation (COV) was 0.24, showing good calculation results.

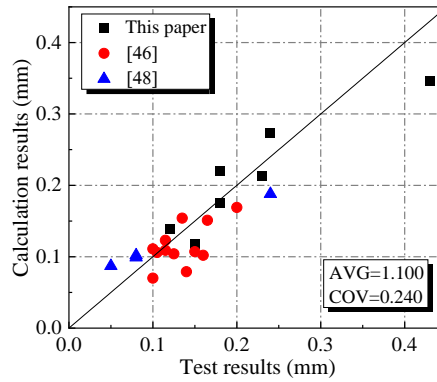


Fig. 12. Comparison between calculation and test maximum crack width of HSSFRC beams.

4.2 Maximum crack width calculation of HSSFRC beam under fatigue load

The cracks in RC members are mainly caused by the strain difference of reinforcement and concrete. The average crack width of RC beams subjected to n fatigue cycles could be calculated as follows:

$$\omega_n = (\overline{\varepsilon_{ns}} - \overline{\varepsilon_{nc}}) l_m \quad (10)$$

where $\overline{\varepsilon_{ns}}$ and $\overline{\varepsilon_{nc}}$ are average strain of reinforcement and concrete after n fatigue cycles within a crack section, respectively; l_m is the average crack spacing of the RC beam.

The tensile reinforcement strain of beams increased rapidly under fatigue loading, while of concrete strain was very small compared with that of the tensile reinforcement. Therefore, for RC beams, the strain of concrete could be ignored when calculating the crack width. The Eq. (10) could be expressed as follows:

$$\omega_n = \overline{\varepsilon_{ns}} l_m = \overline{\phi_s} \overline{\varepsilon_s} l_m \quad (11)$$

where $\overline{\phi_s}$ is strain amplification factor of tensile reinforcement under fatigue loading; $\overline{\varepsilon_s}$ is average strain of tensile reinforcement at first fatigue cycle.

All beams were high-cycle fatigue failure modes in this study. Thus, the material was in the elastic range and the strain distribution of beams in the pure bending region was approximately linear. According to previous research [26], the strain distribution of HSSFRC beam under fatigue loading was still satisfies plane section assumption. Therefore, the following equations could be obtained:

$$\frac{\overline{\varepsilon_s}}{\varepsilon_c} = \frac{h_0 - x}{x} \tag{12}$$

$$\frac{\overline{\varepsilon_{ns}}}{\varepsilon_{nc}} = \frac{h_0 - x_n}{x_n} \tag{13}$$

where ε_c is the strain at the edge of the compressive concrete of HSSFRC beam at first fatigue cycle; x is the depth of the compressive concrete of HSSFRC beam at first fatigue cycle; ε_{nc} is the strain at the edge of the compressive concrete of HSSFRC beam after n fatigue cycles; x_n is the depth of the compressive concrete of HSSFRC beam after n fatigue cycles.

Besides, the depth of compressive concrete for HSSFRC beams basically remains unchanged during the fatigue loading [26], that is $x=x_n$. Therefore, the following equation could be obtained:

$$\overline{\phi_s} = \frac{\overline{\varepsilon_{ns}}}{\varepsilon_s} = \frac{\varepsilon_{nc}}{\varepsilon_c} = \phi_c \tag{14}$$

where ϕ_c is strain amplification factor of HSSFRC under fatigue loading.

According to Eqs. (11) and (14), the expression of maximum crack width of HSSFRC beam after n fatigue cycles could be calculated as follows:

$$\omega_{n,f \max} = \phi_c \omega_{f \max} \tag{15}$$

where $\omega_{f \max}$ is the maximum crack width of the HSSFRC beam at first fatigue cycle and could be calculated through Eq. (8).

Based on Eq. (15), the maximum crack width of the HSSFRC beams subjected to fatigue loading could be obtained through the test results of the strain at the edge of the compressive concrete at different fatigue cycles. However, due to the complexity of fatigue testing and the discreteness of the test results, the Eq. (15) was difficult to apply to the engineering design.

To facilitate engineering application, a simplified empirical formula was proposed in this paper. Zhang [48] reported that the concrete strain amplification factor for SFRC beams is linearly related to the logarithm of fatigue cycles. Through regression analysis of the tested results, it was observed that the strain amplification factor ϕ_c is linearly related to one-third power of the fatigue cycles n for HSSFRC beams. The expression is given as follows:

$$\phi_c = 0.0117n^{1/3} + 0.1566 \tag{16}$$

Substitute Eqs. (8) and (16) into Eq. (15), the empirical formula about the maximum crack width calculation of HSSFRC beam subjected to fatigue loading is given as follows:

$$\omega_{n,f \max} = (0.0117n^{1/3} + 0.1566)(1 - 0.65\lambda_f)\omega_{\max} \tag{17}$$

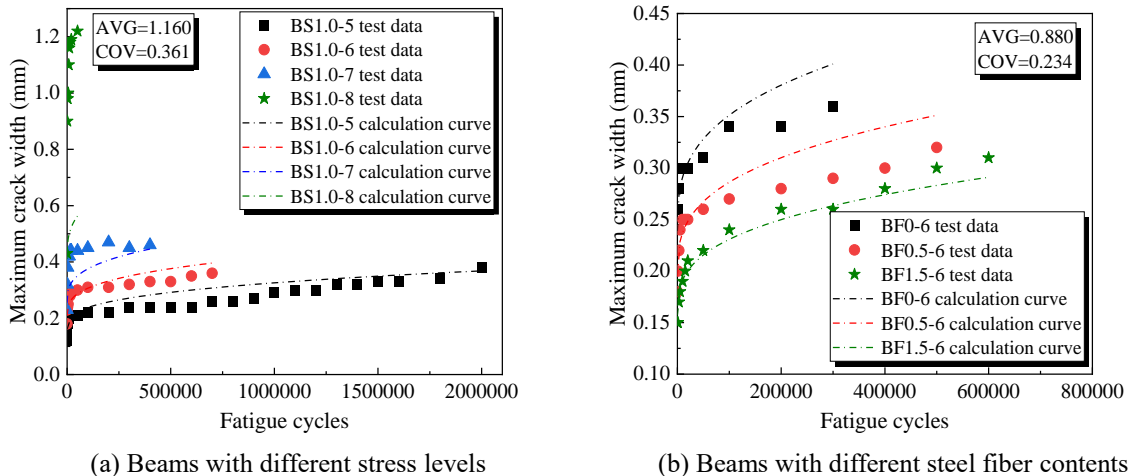


Fig. 13. Comparison between empirical formula calculation curves and test datum of the maximum crack width.

Fig. 13 presents the comparison between empirical formula calculation curves and test datum of the maximum crack width of HSSFRC beams subjected to fatigue loading. As shown, the calculated results exhibited a deviation with the test results, especially for beam BS1.0-8. For beam BS1.0-8, the deviation was attributed to the higher stress level, which may have caused the beam to yield during the fatigue loading. For other beams, the deviation was attributed to the dispersion of the fatigue test results.

5. Midspan deflection calculation of HSSFRC beam

5.1 Midspan deflection calculation of HSSFRC beam under static load

The short-term stiffness calculation formula of reinforced concrete beams under bending moment provided by the standard GB 50010-2010 [45] is given as follows:

$$B = \frac{E_s A_s h_0^2}{1.15\psi + 0.2 + 6\alpha_E \rho / (1 + 3.5\gamma_f')} \tag{18}$$

where ψ is the strain non-uniformity coefficient and can be calculated through Eq. (4); α_E is the ratio of the elastic modulus of longitudinal reinforcement to the elastic modulus of concrete; γ_f' is the ratio of the section area of tension flange to the section area of web, and it taken as 0 for rectangular section beam; ρ is the reinforcement ratio of beam.

Steel fibers could improve the stiffness of beams, therefore, the stiffness calculation formula of SFRC beams subjected to static load could be calculated as follows [38]:

$$B_s = B(1 + \beta_B \lambda_f) \tag{19}$$

where β_B is the influence coefficient of steel fiber.

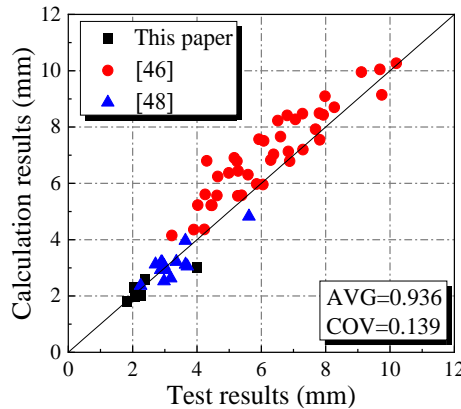


Fig. 14. Comparison between calculation and test midspan deflection of HSSFRC beams.

For SFRC with the strength grade of CF20~CF40, β_B is taken as 0.35 according to the standard [38]. However, it was found that the improvements of steel fiber on stiffness of beams showed a decreasing trend with the increase of concrete compressive strength. This could be explained by that with the increase of concrete strength, the effect of steel fibers on the elastic modulus of concrete gradually decreases. Zhang [48] proposed that β_B is taken as 0.11 for SFRC beams with the concrete strength grade of C60. According to the experimental results in this paper and 11 HSSFRC beams with the concrete strength grade of C80 conducted by Guan [46], the effects of steel fibers on the stiffness improvemet for HSSFRC beams can be negelected. That is to say the stiffness of HSSFRC beam with the concrete strenght grade exceed C80 is approximately equal to that of plain HSC beam with the same concrete strenght grade. Substitute Eq. (19) into Eq. (2), the midspan deflection of HSSFRC beam subjected to static load could be obtained. **Fig. 14** presents the calculation and test midspan deflection of HSSFRC beam under service load in this paper and the related literatures [46, 48]. It could be found that the calculated midspan deflection was relatively large compared with the experimental results of Guan [46]. The main reason was that the concrete strenght grade of some specimens conducted by Guan is between C60~C80, ignoring the influences of steel fiber on stiffness in the calculation process will

result in lower calculated stiffness of these beams, which also means a relatively conservative engineering design.

5.2 Midspan deflection calculation of HSSFRC beam under fatigue load

The stiffness degradation of HSSFRC beams under fatigue loading was mainly owing to the fatigue damage of concrete, tensile reinforcement, and bond degradation between concrete and tensile reinforcement. Through simplification, the Eq. (18) is given as follows:

$$B = \frac{E_s h_0^2}{\frac{1.15\psi + 0.2}{A_s} + \frac{6E_s}{E_c b h_0}} \quad (20)$$

where b is the beam width.

It can be seen from Eq. (20) that the main parameters influencing the stiffness of beams include section size, section area of longitudinal tensile reinforcement, elastic modulus of concrete and reinforcement, and strain non-uniformity coefficient. During the fatigue loading, the section size of beam was remained unchanged. And the applied fatigue load of the beam was lower than its yield strength. Therefore, the tensile reinforcement was in elastic stage and its elastic modulus was also assumed unchanged [49]. Besides, steel fiber can enhance the bond strength between the tensile reinforcement and concrete, and there is almost no bond slip between the tensile reinforcement and concrete during the fatigue loading for SFRC beams [27]. Thus, it could be concluded that the main reasons for the stiffness degradation of HSSFRC beams subjected to fatigue loading were the reduction of tensile reinforcement area and the decreasing of elastic modulus of SFRC. Therefore, the stiffness of HSSFRC beams subjected to fatigue loading could be calculated as follows:

$$B_s^f = \frac{E_s h_0^2}{\frac{1.15\psi + 0.2}{k_1 A_s} + \frac{6E_s}{k_2 E_c b h_0}} \quad (21)$$

where k_1 and k_2 are the degradation coefficients of tensile reinforcement area and SFRC elastic modulus, respectively, which were related to the number of fatigue cycles and steel fiber characteristic parameter.

According to the author's previous research [25, 26], the section area of tensile reinforcement and concrete elastic modulus decreased with the increase in fatigue cycles, while adding steel fibers could significantly decrease their degradation rate. The stiffness degradation rate of SFRC beam subjected to fatigue loading was positively linearly correlated to the logarithm of fatigue cycles, while negatively linearly correlated to the steel fiber characteristic parameter [48]. Therefore, to simplify the calculation, k_1 and k_2 could be calculated as follows:

$$k_1 = k_2 = \frac{a_1 + a_2 \lambda_f}{a_3 + a_4 \lg n} \quad (22)$$

where a_1 , a_2 , a_3 , and a_4 are the undetermined coefficients.

Substitute Eq. (22) into Eq. (21), the stiffness of HSSFRC beam after n fatigue cycles could be obtained:

$$B_s^f = \frac{a_1 + a_2 \lambda_f}{a_3 + a_4 \lg n} B_s \quad (23)$$

By regression analysis on the test stiffness of 12 SFRC beams in the published research [24] and 7 HSSFRC beams in this work, the coefficients a_1 , a_2 , a_3 , and a_4 are taken as 0.88, 0.23, 0.88, and 0.1, respectively. Based on Eqs. (18), (19), (23), and (2), the midspan deflection of HSSFRC beams under fatigue loading could be obtained. **Fig. 15** presents the ratio of the experimental to calculated results of midspan deflection of 19 specimens under different fatigue cycles. As shown, most of the calculation results are between 0.8 and 1.2. Due to the higher stress level applied on the beam BS1.0-8, the beam may yield during the fatigue loading, which results in the calculated midspan deflection smaller than the experimental results.

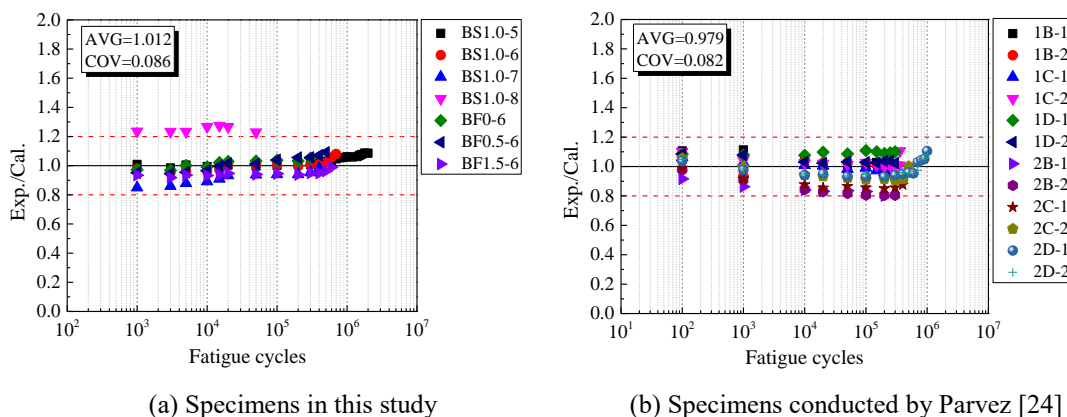


Fig. 15. Comparison between the calculated and experimental midspan deflection of HSSFRC beams.

6. Conclusion

The flexural fatigue behavior of HSSFRC beams was investigated and the calculation methods to predict the midspan deflection and maximum crack width of HSSFRC beams were proposed. The following conclusions can be obtained:

(1) The failure mode of HSSFRC beams under fatigue loading was brittle failure caused by tensile reinforcement fracture. The fatigue life of HSSFRC beams with 0.5%, 1.0%, and 1.5% volume fraction of steel fibers was 37.7%, 106.3%, and 61.4% greater than that of the plain HSC beam, respectively. The optimal steel fiber volume fraction used in engineering for HSC beams subjected to fatigue loading should not exceed 1.0%.

(2) The crack patterns of HSSFRC beams under fatigue loading was better than that of the plain HSC beam. Both the average and maximum crack widths of HSSFRC beams showed a decreasing trend with the increase in steel fiber volume fraction. Compared to HSC beam without steel fibers, the reduction of average crack width of beams with 1.5% volume fraction of steel fibers was exceeded 30%. Steel fibers could effectively restrain the stiffness degradation of HSC beams under fatigue loading.

(3) Under static load, the restraining effects of steel fibers on crack increased with the increase in concrete strength, while the improvement of steel fibers on stiffness decreased with the increase of concrete strength. For HSC beams with the concrete strength grade exceeded C80, the influence of steel fibers on stiffness can be neglected under static load.

(4) The simplified empirical formulas were proposed to predict the midspan deflection and maximum crack width of HSSFRC beams subjected to fatigue loading, and validated by the experimental results.

This paper conducted fatigue tests of HSSFRC beams and verified the effectiveness of steel fiber in improving the fatigue performance of HSC beams. The calculation methods to predict the midspan deflection and maximum crack width were proposed, and the fiber volume fraction applicable for engineering was recommended. The research results presented in this paper could provide reference for design of HSSFRC beams in fatigue loaded structures and facilitate the application of HSSFRC in actual projects. Nevertheless, due to time and test condition limitations, only eight beams were tested in this study, and the proposed calculation methods were empirically fitted based on the specifications. More research is encouraged in the future to enrich the relatively limited experimental results and further validate the proposed empirical formulas.

Acknowledgements

This research is finally supported by National Natural Science Foundation of China (Grant Nos. 51978629 and 52278284), Key Science and Technology Research Project of Henan Province (No. 232102321131), Program for Innovative Research Team of Education Ministry of China (IRT_16R67), and Key Scientific Research Projects of Henan Colleges and Universities (Grant No. 23A570003).

CRedit authorship contribution statement

Zhiqiang Gu: Investigation, Supervision, Conceptualization, Funding acquisition, Writing – original draft. **Hu Feng:** Conceptualization, Formal analysis. **Danying Gao:** Supervision, Investigation, Funding acquisition. **Jun Zhao:** Conceptualization, Supervision, Funding acquisition. **Congjie Wei:** Supervision, Investigation. **Chenglin Wu:** Conceptualization, Supervision.

Conflicts of Interest

The authors declare that they have no known competing financial interests or personal relationships that could have appeared to influence the work reported in this paper.

References

- [1] Moussallam N, Ziegler R, Rudolph J, Bergholz S. A Method for Monitoring Vibrational Fatigue of Structure and Components. *Journal of Pressure Vessel Technology*. Transactions of the ASME 2022; 144(3): 031304. <https://doi.org/10.1115/1.4053380>.
- [2] Zanuy C, Albajar L, Fuente P. Sectional analysis of concrete structures under fatigue loading. *ACI Structural Journal* 2009; 106(5): 667-677. <https://doi.org/10.14359/51663107>.
- [3] Zanuy C, Fuente P, Albajar L. Effect of fatigue degradation of the compression zone of concrete in reinforced concrete sections. *Engineering Structures* 2007; 29(11): 2908-2920. <https://doi.org/10.1016/j.engstruct.2007.01.030>.
- [4] Han JG, Song YP, Wang LC, Song SD, Lei B. Steel Stress Redistribution and Fatigue Life Estimation of Partially Prestressed Concrete Beams under Fatigue Loading. *Advances in Structural Engineering* 2014; 17(2): 179-196. <https://doi.org/10.1260/1369-4332.17.2.179>.
- [5] Zhang WP, Ye ZW, Gu XL, Liu XG, Li SB. Assessment of Fatigue Life for Corroded Reinforced Concrete Beams under Uniaxial Bending. *Journal of Structural Engineering* 2017; 143(7): 04017048. [https://doi.org/10.1061/\(ASCE\)ST.1943-541X.0001778](https://doi.org/10.1061/(ASCE)ST.1943-541X.0001778).
- [6] Wu J, Pang Q, Lv YY, Zhang JP, Gao S. Research on the Mechanical and Physical Properties of Basalt Fiber-Reinforced Pervious Concrete. *Materials (Basel, Switzerland)* 2022; 15(19): 1996-1944. <https://doi.org/10.3390/ma15196527>.
- [7] Wang YG, Gao S, Li W. Study on Compression Deformation and Damage Characteristics of Pine Needle Fiber-Reinforced Concrete Using DIC. *Materials (Basel, Switzerland)* 2022; 15 (5): 1996-1944. <https://doi.org/10.3390/ma15051654>.
- [8] Bencardino F, Rizzuti L, Spadea G, Swamy RN. Implications of test methodology on post-cracking and fracture behaviour of Steel Fibre Reinforced Concrete. *Composites Part B: Engineering* 2013; 46: 31-38. <https://doi.org/10.1016/j.compositesb.2012.10.016>.
- [9] Zhang QY, Xu WW, Sun YC, Ji YC. Investigation on Mechanical and Microstructure Properties of Steel Fiber Reinforced Concrete. *Advances in Materials Science and Engineering* 2022; (2022). <https://doi.org/10.1155/2022/3681132>.
- [10] Thomas J, Ramaswamy A. Mechanical Properties of Steel Fiber-Reinforced Concrete. *Journal of Materials in Civil Engineering* 2008; 19(5): 385-392. [https://doi.org/10.1061/\(ASCE\)0899-1561\(2007\)19:5\(385\)](https://doi.org/10.1061/(ASCE)0899-1561(2007)19:5(385)).
- [11] Niu YF, Huang HL, Wei JX, Jiao CJ, Miao QQ. Investigation of fatigue crack propagation behavior in steel fiber-reinforced ultra-high-performance concrete (UHPC) under cyclic flexural loading. *Composite Structures* 2022; (282). <https://doi.org/10.1016/j.compstruct.2021.115126>.
- [12] Al-Damad IMA, Foster SJ. Behavior of Postcracked steel fiber-reinforced concrete in fatigue and development of a damage prediction model. *Structure Concrete* 2022; 23(3): 1593-1610. <https://doi.org/10.1002/suco.202100497>.
- [13] Zhang J, Stang H. Fatigue performance in flexure of fiber reinforced concrete. *ACI Materials Journal* 1998; 95(1):58-67. <https://doi.org/10.14359/351>.
- [14] Goel S, Singh SP. Fatigue performance of plain and steel fibre reinforced self compacting concrete using S–N relationship. *Engineering Structural* 2014; 74: 65-73. <https://doi.org/10.1016/j.engstruct.2014.05.010>.
- [15] Singh SP, Kaushik SK. Fatigue strength of steel fibre reinforced concrete in flexure. *Cement and Concrete Composites* 2003; 25 (7): 779-786. [https://doi.org/10.1016/S0958-9465\(02\)00102-6](https://doi.org/10.1016/S0958-9465(02)00102-6).
- [16] Singh SP, Mohammadi Y, Madan SK. Flexural fatigue strength of steel fibrous concrete containing mixed steel fibres. *Journal of Zhejiang University - Science A* 2006; 7(8): 1329-1335.
- [17] Isojeh B, El-Zeghayar M, Vecchio FJ. Fatigue Behavior of Steel Fiber Concrete in Direct Tension. *Journal of Materials in Civil Engineering* 2017; 29(9): 04017130. [https://doi.org/10.1061/\(ASCE\)MT.1943-5533.0001949](https://doi.org/10.1061/(ASCE)MT.1943-5533.0001949).
- [18] Zhang HH, Xiao JZ, Tang YX, Duan ZH, Poon CS. Long-term shrinkage and mechanical properties of fully recycled aggregate concrete: Testing and modelling. *Cement and Concrete Composites* 2022; 130: 104527. <https://doi.org/10.1016/j.cemconcomp.2022.104527>.

- [19] Zhao QH, Wang YQ, Xie M, Huang BS. Experimental study on mechanical behavior of steel fiber reinforced geopolymeric recycled aggregate concrete. *Construction and Building Materials* 2022; 356: 129267. <https://doi.org/10.1016/j.conbuildmat.2022.129267>.
- [20] Gao DY, Zhang LJ, Nokken M. Mechanical behavior of recycled coarse aggregate concrete reinforced with steel fibers under direct shear. *Cement and Concrete Composites* 2017; 79: 1-8. <https://doi.org/10.1016/j.cemconcomp.2017.01.006>.
- [21] Gao DY, Gu ZQ, Pang YY, Yang L. Mechanical properties of recycled fine aggregate concrete incorporating different types of fibers. *Construction and Building Materials* 2021; 298: 123732. <https://doi.org/10.1016/j.conbuildmat.2021.123732>.
- [22] Gao DY, Zhang LJ. Flexural performance and evaluation method of steel fiber reinforced recycled coarse aggregate concrete. *Construction and Building Materials* 2018; 159: 126-136. <https://doi.org/10.1016/j.conbuildmat.2017.10.073>.
- [23] Tan Y, Zhou CX, Zhou JZ. Influence of the Steel Fiber Content on the Flexural Fatigue Behavior of Recycled Aggregate Concrete. *Advances in Civil Engineering* 2020; 2020: 8839271. <https://doi.org/10.1155/2020/8839271>.
- [24] Parvez A, Foster SJ. Fatigue Behavior of Steel-Fiber-Reinforced Concrete Beams. *Journal of Structural Engineering* 2015; 141(4): 04014117. [https://doi.org/10.1061/\(ASCE\)ST.1943-541X.0001074](https://doi.org/10.1061/(ASCE)ST.1943-541X.0001074).
- [25] Gao DY, Gu ZQ, Tang JY, Zhang C. Fatigue performance and stress range modeling of SFRC beams with high-strength steel bars. *Engineering Structures* 2020; 216: 110706. <https://doi.org/10.1016/j.engstruct.2020.110706>.
- [26] Gao DY, Gu ZQ, Zhu HT, Huang YB. Fatigue behavior assessment for steel fiber reinforced concrete beams through experiment and Fatigue Prediction Model. *Structures* 2020; 27: 1105-1117. <https://doi.org/10.1016/j.istruc.2020.07.028>.
- [27] Isojeh B, El-Zeghayar M, Vecchio FJ. Fatigue Resistance of Steel Fiber-Reinforced Concrete Deep Beams. *ACI Structural Journal* 2017; 114(5). <https://doi.org/10.14359/51700792>.
- [28] Isojeh B, El-Zeghayar M, Vecchio FJ. High-cycle fatigue life prediction of reinforced concrete deep beams. *Engineering Structures* 2017; 150: 12-24. <https://doi.org/10.1016/j.engstruct.2017.07.031>.
- [29] Mohamed Adel, Koji M, Tamon U, Kohei N. Material comparative analysis of crack-bridging degradation of SFRC structural beams under flexural fatigue loading. *Construction and Building Materials* 2022; 339: 127642. <https://doi.org/10.1016/j.conbuildmat.2022.127642>.
- [30] Pereira Prado L, Carrazedo R, Khalil EDM. Interface strength of High-Strength concrete to Ultra-High-Performance concrete. *Engineering Structures* 2022; 252. <https://doi.org/10.1016/j.engstruct.2021.113591>.
- [31] Gao DY, Huang YC, Yuan JS, Gu ZQ. Probability distribution of bond efficiency of steel fiber in tensile zone of reinforced concrete beams. *Journal of Building Engineering* 2021; 43: 102550. <https://doi.org/10.1016/j.jobbe.2021.102550>.
- [32] Kara IF, Dundar C. Prediction of deflection of high strength steel fiber reinforced concrete beams and columns. *COMPUTERS AND CONCRETE* 2012; 9(2): 133-151. <https://doi.org/10.12989/cac.2012.9.2.133>.
- [33] Liu HB, Xiang TY, Zhao RD. Research on non-linear structural behaviors of prestressed concrete beams made of high strength and steel fiber reinforced concretes. *Construction and Building Materials* 2009; 23(1): 85-95. <https://doi.org/10.1016/j.conbuildmat.2008.01.016>.
- [34] Dancygier AN, Savir Z. Effects of Steel Fibers on Shear Behavior of High-Strength Reinforced Concrete Beams. *Advances in Structural Engineering* 2011; 14(5): 745-762. <https://doi.org/10.1260/1369-4332.14.5.745>.
- [35] Tahenni T, Chemrouk M, Lecompte T. Effect of steel fibers on the shear behavior of high strength concrete beams. *Journal of Engineering and Applied Sciences* 2016; 105: 14-28. <https://doi.org/10.36478/jeasci.2020.2758.2766>.
- [36] Yoo DY, Yang JM. Effects of stirrup, steel fiber, and beam size on shear behavior of high-strength concrete beams. *Cement & Concrete Composites* 2018; 87(8): 137-148. <https://doi.org/10.1016/j.cemconcomp.2017.12.010>.
- [37] ACI 318. Building code requirements for structural concrete and commentary, American Concrete Institute, Farmington Hills, MI, 2011.
- [38] CECS 38: 2004, Technical specification for fiber reinforced concrete structures, Standards of China Association of Engineering Construction, 2004.
- [39] Song L, Yu ZW. Fatigue performance of corroded reinforced concrete beams strengthened with CFRP sheets. *Construction and Building Materials* 2015; 90: 99-109. <https://doi.org/10.1016/j.conbuildmat.2015.05.024>.
- [40] Saikali RE, Pantazopoulou SJ, Palermo D. Local Bond-Slip Behavior of Reinforcing Bars in High-Performance Steel Fiber-Reinforced Concrete Beams. *ACI Structural Journal* 2022; 119: 139-153. <https://doi.org/10.14359/51734334>.
- [41] Gao DY, Gu ZQ, Wei CJ, Wu CL, Pang YY. Effects of fiber clustering on fatigue behavior of steel fiber

- reinforced concrete beams. *Construction and Building Materials* 2021; 301: 124070. <https://doi.org/10.1016/j.conbuildmat.2021.124070>.
- [42] Mousavi SR, Esfahani MR. Effective Moment of Inertia Prediction of FRP-Reinforced Concrete Beams Based on Experimental Results. *Journal of Composites for Construction* 2012; 16(5): 490-498. [https://doi.org/10.1061/\(ASCE\)CC.1943-5614.0000284](https://doi.org/10.1061/(ASCE)CC.1943-5614.0000284).
- [43] Hua YT, Yin SP, Peng ZT. Crack development and calculation method for the flexural cracks in BFRP reinforced seawater sea-sand concrete (SWSSC) beams. *Construction and Building Materials* 2020; 255. <https://doi.org/10.1016/j.conbuildmat.2020.119328>.
- [44] Yao XH, Guan JF, Zhang L, Xi JY, Li LL. A Unified Formula for Calculation of Crack Width and Spacing in Reinforced Concrete Beams. *International Journal of Concrete Structures and Materials* 2021; 15(1): 1-28. <https://doi.org/10.1186/s40069-021-00479-4>.
- [45] GB 50010, Code for design of concrete structures, National Standards of the People's Republic of China, 2010.
- [46] Q. Guan, 2005. Research on flexural behavior of steel fiber reinforced high-strength concrete beams, Zhengzhou University, 2005.
- [47] Michel A, Solgaard AOS, Pease BJ, Geiker MR, Stang H, Olesen JF. Experimental investigation of the relation between damage at the concrete-steel interface and initiation of reinforcement corrosion in plain and fibre reinforced concrete. *Corrosion Science* 2013; 77: 308-321. <https://doi.org/10.1016/j.corsci.2013.08.019>.
- [48] M. Z, 2015. Fatigue Performance and Calculation Method of Steel Fiber Reinforced High-strength Concrete Beams, Zhengzhou University, 2015.
- [49] Fadi O, Raafat EH. Analytical fatigue prediction model of RC beams strengthened in flexure using prestressed FRP reinforcement. *Engineering Structures* 2013; 46: 173-183. <https://doi.org/10.1016/j.engstruct.2012.07.020>.